Calculation of the wide-angle neutron spectra from the ^{9}Be(d, xn) reaction in a thick beryllium target*

Zheng Wei(韦峥)[1,2;1)] Jun-Run Wang(王俊润)[1,2] Ya-Ling Zhang(张雅玲)[1,3] Zhi-Wu Huang(黄智武)[1]
Zhan-Wen Ma(马占文)[1] Jie Zhang(张杰)[1] Yan-Yan Ding(丁琰琰)[1] Li Xia(夏莉)[1] Jian-Yi Li(李建一)[1]
Xiao-Long Lu(卢小龙)[1,2] Yu Zhang(张宇)[1,2] Da-Peng Xu(徐大鹏)[1,2] Lei Yang(杨磊)[3] Ze-En Yao(姚泽恩)[1,2;2)]

[1]School of Nuclear Science and Technology, Lanzhou University, Lanzhou 730000, China
[2]Engineering Research Center for Neutron Application, Ministry of Education, Lanzhou University, Lanzhou 730000, China
[3]Institute of Modern Physics, Chinese Academy of Sciences, Lanzhou 730000, China

Abstract: The multi-layer computing model is developed to calculate wide-angle neutron spectra, in the range from 0° to 180° with a 5° step, produced by bombarding a thick beryllium target with deuterons. The double-differential cross-sections (DDCSs) for the ^{9}Be(d, xn) reaction are calculated using the TALYS-1.8 code. They are in agreement with the experimental data, and are much better than the PHITS-JQMD/GEM results at 15° , 30° , 45° and 60° neutron emission angles for deuteron energy of 10.0 MeV. In the TALYS-1.8 code, neutron contributions from direct reactions (break-up, stripping and knock-out reactions) are controlled by adjustable parameters, which describe the basic characteristics of typical direct reactions and control the relative intensity and the position of the ridgy hillock at the tail of DDCSs. It is found that the typical calculated wide-angle neutron spectra for different neutron emission angles and neutron angular distributions agree quite well with the experimental data for 13.5 MeV deuterons. The multi-layer computing model can reproduce the experimental data reasonably well by optimizing the adjustable parameters in the TALYS-1.8 code. Given the good agreement with the experimental data, the multi-layer computing model could provide better predictions of wide-angle neutron energy spectra, neutron angular distributions and neutron yields for the ^{9}Be(d, xn) reaction neutron source.

Keywords: neutron source, ^{9}Be(d, xn) reaction, thick target, wide-angle neutron spectra, neutron angular distributions

PACS: 25.45.-z, 29.87.+g, 29.27.Fh **DOI:** 10.1088/1674-1137/43/5/054001

1 Introduction

In recent decades, a lot of attention has been focused on various properties of high-current accelerator-based neutron sources that are based on deuteron bombardment of thick targets of light elements [1-12]. The ^{2}H(d,n)^{3}He, ^{3}H(d,n)^{4}He, ^{7}Li(d,n)^{8}Be and ^{9}Be(d,xn) reactions, as typical direct reactions, are included. The characteristics of the ^{2}H(d,n)^{3}He and ^{3}H(d,n)^{4}He reactions in thick targets, including the neutron energy spectra, neutron angular distributions and neutron yields, have been widely investigated due to their importance for producing quasi-monoenergetic neutrons with low energy deuterons [4, 5]. The ^{7}Li(d,n)^{8}Be and ^{9}Be(d,xn) neutron sources produce continuous-spectrum neutron fields [8, 12], which are very useful for applications such as in radiobiology [13], radiotherapy [14, 15], radiography [16, 17] and materials research [18]. To develop an accelerator-based neutron source for these applications, detailed information on the overall intensity and the emitted-neutron energy spectrum is necessary.

Deuterons are used to bombard a beryllium-metal target that is thick enough to stop the incident deuterons so as to produce intense, continuous-spectrum neutron fields. In the case of low energy deuterons, ^{9}Be(d,n)^{10}B is

Received 31 October 2018, Revised 18 February 2019, Published online 11 March 2019

* Supported by the National Magnetic Confinement Fusion Science Program of China (2014GB104002), the National Natural Science Foundation of China (11705071, 11875155, 11675069, 21327801), NSAF (U1830102), the National Key Scientific Instrument and Equipment Development Project (2013YQ40861), and the Fundamental Research Funds for the Central Universities (lzujbky-2017-13, lzujbky-2017-kb09)

1) E-mail: weizheng@lzu.edu.cn
2) E-mail: zeyao@lzu.edu.cn

an exothermic reaction with Q=+4.36 MeV, but the produced neutron spectrum has a characteristic of a continuous-spectrum because of the four well-known excited states of ^{10}B [12, 19]. For higher incident energies, the reactions ^{9}Be(d,2n)^{9}B with Q=−4.1 MeV, ^{9}Be(d,np)^{9}Be with Q=−2.2 MeV, ^{9}Be(d,2np)^{8}Be with Q=−3.8 MeV, and so on, can also be used to produce neutrons, and they markedly enhance the neutron yields and extend the neutron energy spectrum in a ^{9}Be(d,xn) neutron source.

It is important to use a thick beryllium-metal targets for an accelerator-based neutron source, because the beryllium-metal target has various advantages over gaseous or liquid targets, including chemical stability, higher melting point (1280℃) and better thermal conductivity, which allow to withstand high beam currents of several mA. As a result, the accelerator-based ^{9}Be(d,xn) reaction neutron source can provide high intensity and continuous-spectrum neutron fields.

In this work, the multi-layer computing model has been developed for calculating the neutron energy spectrum, neutron angular distributions and neutron yields of the ^{9}Be(d,xn) reaction neutron source with a thick beryllium target. The emphasis of this work is to evaluate and provide detailed information on the wide-angle neutron spectra for different neutron emission angles.

2 Multi-layer computing model

In the ^{9}Be(d,xn) reaction neutron source, deuterons bombard a beryllium-metal target that is thick enough to completely stop the incident deuterons so as to produce intense and continuous-spectra neutron fields. The neutron energy spectrum from this source in different emission directions can be represented as

$$\frac{\mathrm{d}Y_n^2}{\mathrm{d}\Omega\cdot\mathrm{d}E_n}(\theta,E_n,E_{dI})=\int_{E_{dI}}^{0} I_0 N_d \frac{\mathrm{d}^2\sigma}{\mathrm{d}\Omega\cdot\mathrm{d}E_n}(\theta,E_n,E_d)\times\frac{1}{S(E_d)}\cdot\mathrm{d}E_d, \tag{1}$$

where I_0 denotes the intensity of incident deuterons and E_{dI} is the incident energy. E_d is the deuteron energy in the target, N_d the atomic density of beryllium-metal target, E_n the neutron energy, and θ the neutron emission angle. $\frac{\mathrm{d}^2\sigma}{\mathrm{d}\Omega\cdot\mathrm{d}E_n}$ is the DDCS of the ^{9}Be(d,xn) reaction. $S(E_d)=-\frac{\mathrm{d}E_d}{\mathrm{d}x(E_d)}$ denotes the stopping power of deuterons in beryllium-metal, which is computed by the SRIM-2010 code [20]. All physical quantities are given in the lab system.

There are no experimental data for the stopping power of deuterons in beryllium-metal, but the stopping power data for protons in beryllium-metal, calculated by the SRIM-2010 code, are 11.65% lower than the experimental results [21, 22]. From the considerations of uncertainty of SRIM-2010 [20], we estimate that the uncertainty of SRIM-2010 calculations of the stopping power of deuterons in beryllium-metal target is about 11.65%. The uncertainty data from SRIM-2010 is not used for compensating the calculations in this work.

According to the multi-layer computing model, the thick beryllium-metal target should be divided into thinner layers when calculating the neutron energy spectrum. Consequently, in every layer, the neutron energy spectrum is obtained by

$$\frac{\mathrm{d}Y_{n,i}^2}{\mathrm{d}\Omega\cdot\mathrm{d}E_n}(\theta,E_n,E_{d,i})=I_0 N_d \frac{\mathrm{d}^2\sigma}{\mathrm{d}\Omega\cdot\mathrm{d}E_n}(\theta,E_n,E_{d,i})\times\frac{1}{S(E_{d,i})}\cdot\Delta E_{d,i}. \tag{2}$$

where $E_{d,i}$ denotes the deuteron energy in the $i-th$ layer, i is the index of the layer, and $\Delta E_{d,i}$ the energy loss of deuterons in the i-th layer. The neutron energy spectrum for a thick target is derived as

$$\frac{\mathrm{d}Y_n^2}{\mathrm{d}\Omega\cdot\mathrm{d}E_n}(\theta,E_n,E_{dI})=\sum_i \frac{\mathrm{d}Y_{n,i}^2}{\mathrm{d}\Omega\cdot\mathrm{d}E_n}(\theta,E_n,E_{d,i}). \tag{3}$$

In the case of $E_{d,0}=E_{dI}$ and $\Delta E_{d,0}=0$, $E_{d,i}$, $\Delta E_{d,i}$ can be computed by

$$E_{d,i}=E_{d,i-1}-\Delta E_{d,i-1}, \tag{4}$$

$$\Delta E_{d,i-1}=S(E_{d,i-1})\cdot\Delta x_{i-1}, \tag{5}$$

where Δx_{i-1} denotes the thickness of the $(i-1)-th$ layer.

For the neutron-emission direction θ , the differential neutron yield can be obtained by integrating Eq. (3), and is given as

$$\frac{\mathrm{d}Y_n}{\mathrm{d}\Omega}(\theta,E_{dI})=\int_{E_{\min}}^{E_{\max}} \frac{\mathrm{d}Y_n^2}{\mathrm{d}\Omega\cdot\mathrm{d}E_n}(\theta,E_n,E_{dI})\cdot\mathrm{d}E_n, \tag{6}$$

where $E_{\max}$ denotes the maximum neutron energy, and $E_{\min}$ is the minimum neutron energy. The distribution of differential neutron yield for different neutron emission angles is called neutron angular distribution.

Deuterons with energies of several MeV that bombard a thick beryllium target are particularly favored for an intense neutron source. However, experimental measurements of the cross-section of the ^{9}Be(d,xn) reaction is an arduous work, in particular for DDCSs. The TALYS code was developed by combining several nuclear reaction models, ranging from the direct reaction process, compound nucleus process to complex-particle pre-equilibrium process and multiple particle emission process, which can be used to calculate DDCSs. The ^{9}Be(d,xn) reaction can be calculated with the TALYS-1.8 code [23] to include typical direct reaction processes, such as projectile break-up, stripping and knock-out.

The break-up, stripping and knock-out contributions can be adjusted with the Cbreak, Cstrip and Cknock

keywords in the TALYS-1.8 code [23]. DDCSs of the ^{9}Be(d, xn) reaction for different emission angles were calculated by the TALYS-1.8 code. We have compared all published experimental DDCSs with our calculated results for the ^{9}Be(d, xn) reaction at energies of 8.8 MeV (neutron emission angle θ =3.5°), 10.0 MeV (θ =15°, 30°, 45°, 60°) and 18.1 MeV (θ =3.5°), and found that the calculated results are in agreement with the experimental DDCSs. Fig. 1 shows a typical result for DDCSs, corresponding to 10.0 MeV incident deuterons and neutron emission angles ranging from 0° to 180° with a 5° step. The parameters, such as Cbreak, Cstrip, Cknock, avadjust, rvadjust, gnadjust, gpadjust, avdadjust, awdadjust, etc., were adjusted so as to optimize the calculation results.

Figure 2 shows the calculated DDCSs in this work and the experimental data [24], our previous calculated results [12], and PHITS-JQMD/GEM results [25] at 15°, 30°, 45° and 60° emission angles for deuterons of 10.0 MeV. The calculated results in this work agree quite well with the experimental data and with the other calculated results. One can also see that the calculated results in this work are closer to the experimental data than our previous calculated results [12], especially for low energy neutrons. This shows that the calculated results using the new set of parameters reasonably represent DDCSs of the

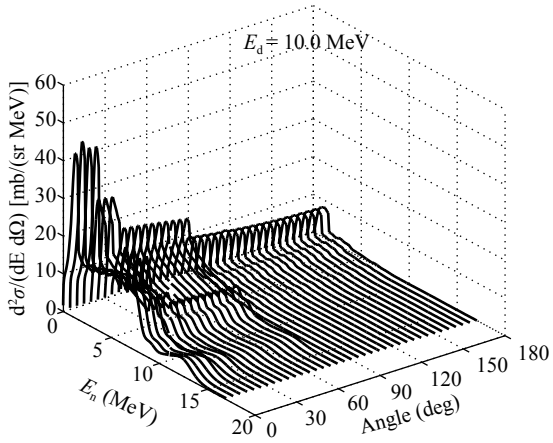

Fig. 1. Calculated DDCSs for the ^{9}Be(d, xn) reaction using the TALYS-1.8 code for incident deuterons with an energy of 10.0 MeV.

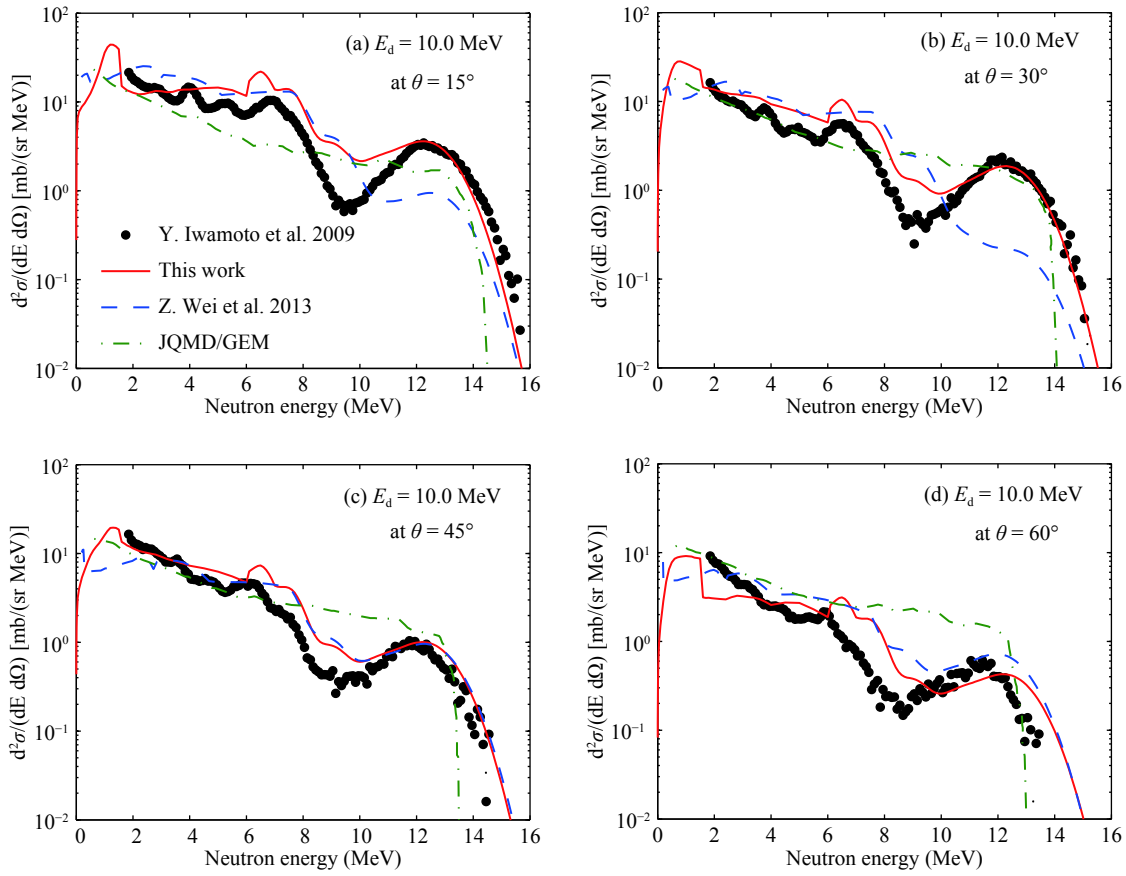

Fig. 2. (color online) The comparison of the calculated DDCSs and the experimental data for deuterons at 10.0 MeV and emission angles of θ =15°, 30°, 45° and 60°. The scattered symbols denote the experimental data [24]. The red solid curves denote the calculated DDCSs by the TALYS-1.8 code in this work, the blue dashed curves denote the previously calculated DDCSs by TALYS-1.4 code, and the green dot-dashed curves denote the calculated DDCSs by PHITS-JQMD/GEM.

^{9}Be(d, xn) reaction.

According to the comparison between the calculated DDCSs of the ^{9}Be(d, xn) reaction and the experimental data for 10.0 MeV deuterons in Fig. 2, one can see a well pronounced bell-like shape at the tail end [3], which comes from neutrons from direct reactions, including break-up, stripping and knock-out reactions. The neutrons from direct reactions enhance the neutron yields at forward angles in the ^{9}Be(d, xn) neutron source. Neutrons from direct reactions are still visible at larger angles, but the relative intensity and the position of the maxima decrease with the angle.

The developed multi-layer mode can be used to calculate the wide-angle neutron energy, neutron angular distributions and neutron yields of the ^{9}Be(d, xn) reaction with a thick beryllium target by using DDCSs of the ^{9}Be(d, xn) reaction calculated by the TALYS-1.8 code and the stopping power calculated by SRIM-2010.

3 Results and discussions

In this work, we developed the multi-layer computing model, according to Eqs. (2)-(5), to study the wide-angle characteristics of the ^{9}Be(d, xn) reaction neutron source with a thick beryllium target at different neutron emission angles. The stopping power is calculated by the SRIM-2010 code and DDCSs are computed by the TALYS-1.8 code, which are invoked in the multi-layer computing model.

As an example, we calculated the wide-angle neutron spectra for the ^{9}Be(d, xn) reaction with 13.5 MeV deuterons and compared them with the experimental data. From the experimental data for 13.54 MeV deuterons, the range of deuterons in beryllium-metal is about 0.784 mm, and therefore, the thickness of the beryllium-metal target is 0.784 mm in this work.

Figure 3 shows the calculated wide-angle neutron spectra for angles in the range from 0° to 180° with a 5° step. The calculated results are compared with the experimental data [26] in Fig. 4. It is noted that the calculated results agree quite well with the experimental data.

In Fig. 4, it is obvious that the experimental data are still higher than the calculated results for neutron energies lower than 2.0 MeV. In particular, a small peak is observed in the experimental spectra near the neutron energy of 0.8 MeV at every emission angle. This small peak arises from the typical inelastic scattering reaction, ^{9}Be(d, d′)^{9}Be$*$ [12]. It is noted that ^{9}Be$*$ is in an excited state with the energy of 2.43 MeV, and it decays into ^{8}Be by emitting a neutron with the energy of 0.8 MeV, namely, ^{9}Be(d, d′)^{9}Be$* \rightarrow {}^{8}\mathrm{Be} + \mathrm{n}$. Importantly, one can also see a ridgy hillock at the tail end, particularly for small forward angles, which has the characteristics of DDCSs of the ^{9}Be(d, xn) reaction. These neutrons are produced in

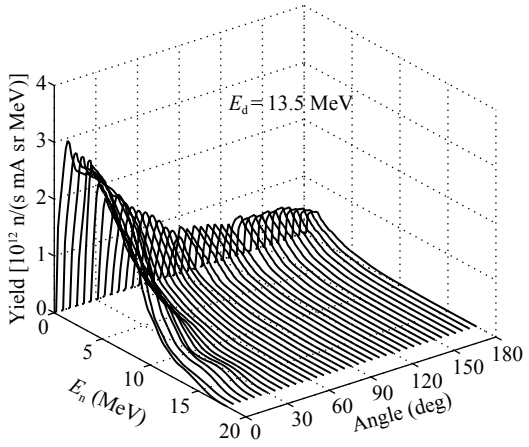

Fig. 3. Wide-angle neutron energy spectra of the ^{9}Be(d, xn) reaction neutron source for incident deuterons with energy of 13.5 MeV for a thick beryllium target.

direct-like reactions, including break-up, stripping and knock-out reactions. Neutrons from direct reactions enhance the neutron yields at forward angles in the ^{9}Be(d, xn) neutron source. As the angle increases, this hillock is gradually blurred. Neutrons from direct reaction mechanisms are still visible at larger angles, but the relative intensity and the position of the maxima decrease with the angle.

According to Eq. (6), neutron yields for angles ranging from 0° to 180° with a 5° step are calculated and shown in Fig. 5 for the ^{9}Be(d, xn) neutron source with a thick beryllium-metal target at deuteron incident energy of 13.5 MeV . The experimental data is also shown for comparison. Obviously, the calculated results agree with the experimental data very well, which indicates that the multi-layer computing model can calculate and evaluate the ^{9}Be(d, xn) reaction reasonably well. Notably, the neutron yield at very forward angles is higher for the ^{9}Be(d, xn) neutron source, which is due to the contributions of direct reactions (break-up, stripping and knock-out reactions).

4 Conclusion

In this work, the multi-layer computing model has been developed to calculate and evaluate the wide-angle neutron energy spectra, neutron angular distributions and neutron yields for the ^{9}Be(d, xn) reaction neutron source with a thick beryllium target. For typical experimental data for deuterons with energy of 13.54 MeV, the calculated results are compared with the experimental data, and are in very good agreement.

^{9}Be(d, xn) reaction is a typical direct reaction process for which one can see a ridgy hillock at the tail end in DDCSs or neutron spectra distributions, in particular for small forward angles. Neutron contributions from direct

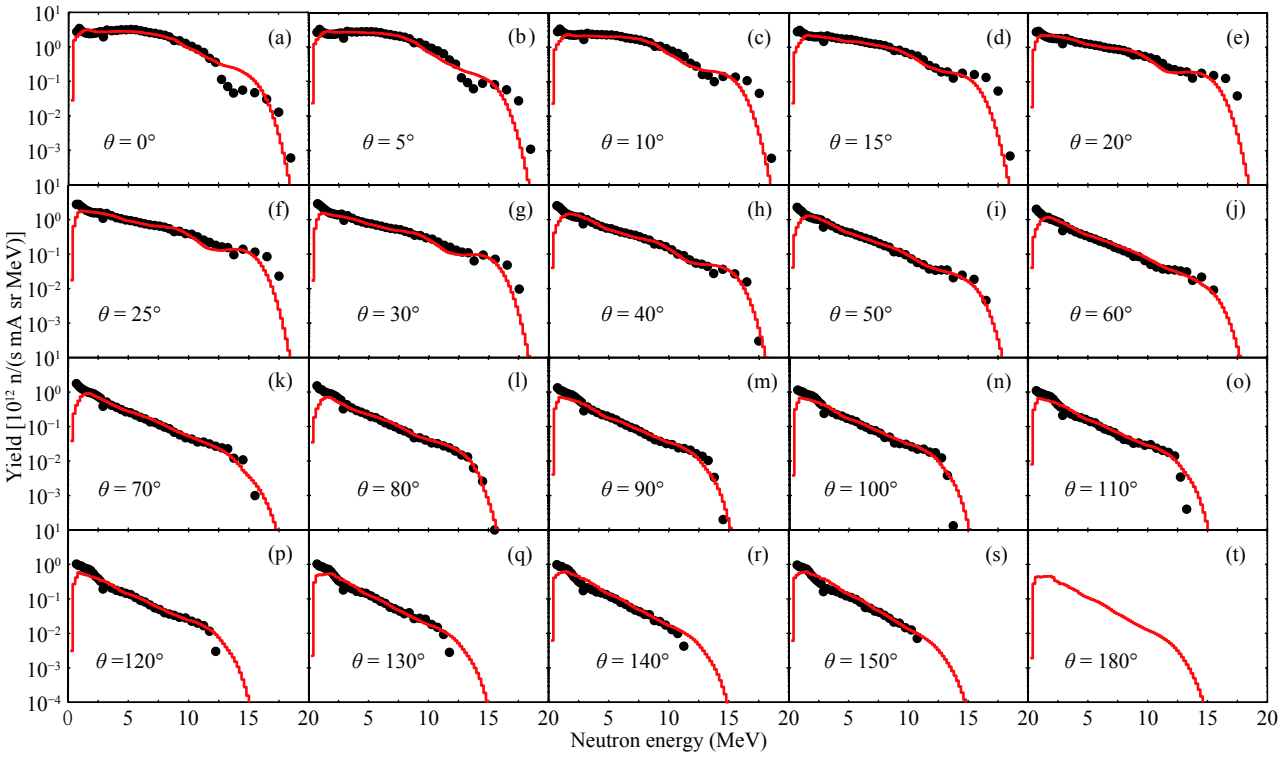

Fig. 4. (color online) The comparison of the calculated neutron spectra and the experimental data at different neutron emission angles. The circle symbols denote the experimental data (13.54 MeV deuterons), taken from Ref. [26]. The thickness of the beryllium target is 2.0 mm. The red solid curves denote the calculated results at neutron emission angles ranging from 0° to 180°.

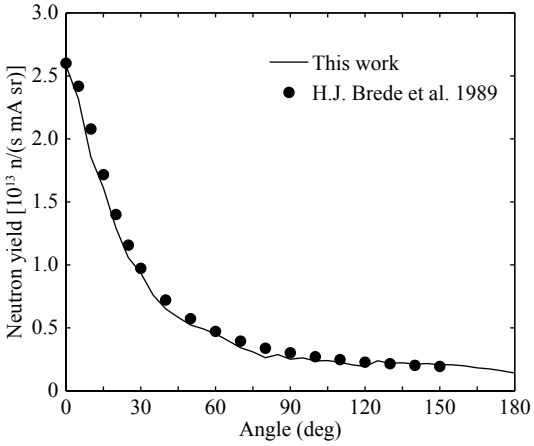

Fig. 5. Angular distribution of neutrons from the ^{9}Be(d,xn) neutron source with a thick beryllium target. The solid curve denotes the calculated results in this work, and the circle symbols are the experimental data [26] for deuteron energy of 13.54 MeV and recoil proton energy threshold of E_{th}=2 MeV.

reactions, including break-up, stripping and knock-out reactions, enhance the neutron yields at small forward angles for the ^{9}Be(d,xn) neutron source. Neutron contributions from direct reaction mechanisms are still visible at higher angles, but the relative intensity and the position of the maxima decrease with the angle.

The calculated DDCSs of the ^{9}Be(d,xn) reaction obtained with the TALYS-1.8 code have a number of uncertainties, which rely on the relevant adjustable parameters. Consequently, the deviation of the calculated neutron spectra mainly stem from the uncertainties of DDCSs. The calculated DDCSs in this work are in good agreement with the experimental data, owing to the increased effect of direct reaction processes. The multi-layer computing model works very well for calculating the wide-angle neutron energy spectra, neutron angular distributions and neutron yields for the ^{9}Be(d,xn) reaction neutron source with a thick beryllium target. Given the good agreement with the existing data, the multi-layer computing model should provide better predictions of wide-angle neutron energy spectra, neutron angular distributions and neutron yields for the ^{9}Be(d,xn) reaction neutron source for deuteron energy regions where data is not available. The multi-layer computing model can be used to evaluate the wide-angle characteristics of the ^{9}Be(d,xn) reaction with a thick beryllium target in the accelerator-based neutron sources and for other applications.

We are grateful to Dr. Koning for guiding the TALYS in adjusting the main parameters for direct reactions.

References

1 V. V. Shirokov, A. A. Babkin, P. V. Bykov et al, Proceeding of EPAC, Lucerne, Switzerland (2004)
2 L. Oláh, A. M. El-Megrab, A. Fenyvesi et al, Nucl. Instrum. Methods Phys. Res. A, **404**: 373 (1998)
3 Z. Radivojevic, A. Honkanen, J. Äystö, V. Lyapin, V. Rubchenya, W. H. Trazska, D. Vakhtin, and G. Walter, Nucl. Instrum. Methods Phys. Res. B, **183**: 212 (2001)
4 Z. E. Yao, H. X. Du, X. J. Tan, Y. Zhang, K. Tooru, and B. Gerard, Chinese Journal of Computational Physics, **25**: 744 (2008)
5 Z. E. Yao, W. M. Yue, P. Luo, X. J. Tan, H. X. Du, and Y. B. Nie, Atomic Energy Science and Technology, **42**: 400 (2008)
6 X. Z. Wang, X. X Bai, A. L. Li, W. P. Liu, D. H. Qi, Y. Yuan, and G. J. Si, Nuclear Science and Techniques, **5**: 193 (1994)
7 M. A. Lone, C. B. Bigham, J. S. Fraser, H. R. Schneider, T. K. Alexander, A. J. Ferguson, and A. B. McDonald, Nucl. Instrum. Methods, **143**: 331 (1977)
8 M. Baba, T. Aoki, M. Hagiwara, M. Sugimoto, T. Miura, N. Kawata, A. Yamadera, and H. Orihara, Journal of Nuclear Materials, **307**: 1715 (2002)
9 G. á. Sziki, A. Simon, Z. Szikszai, Zs. Kertész, and E. Dobos, Nucl. Instrum. Methods Phys. Res. B, **251**: 343 (2006)
10 L. Oláh, A. Fenyvesi, J. Jordanova, A. M. El-Megrab, A. D. Majdeddin, Darsono, N. Perez, M. Y. A. Yousif, and J. Csikai, Applied Radiation and Isotopes, **50**: 479 (1999)
11 J. F. Zhang, X. C. Ruan, L. Hou, X. Li, G. G. Zhang, J. Bao, H. X. Huang, and Y. B. Nie, High Power Laser and Particle Beams, **23**: 209 (2011)
12 Z. Wei, Y. Yan, Z. E. Yao, C. L. Lan, and J. Wang, Physical Review C, **87**: 054605 (2013)
13 J. P. Meulders, P. Leleux, P. C. Macq, and C. Pirart, Phys. Med. Biol., **20**: 235 (1975)
14 N. Colonna, L. Beaulieu, L. Phair, G. J. Wozniak, L. G. Moretto, W. T. Chu, and B. A. Ludewigt, Med. Phys., **26**: 793 (1999)
15 T. E. Blue and J. C. Yanch, Journal of Neuro-Oncology, **62**: 19 (2003)
16 Y. B. Zou, Y. Y. Pei, D. W. Mo, G. Y. Tang, J. M. Guo, J. G. Xu, G. H. Zhang, and Z. Y. Guo, FNDA, 058 (2006) http://cds.cern.ch/record/1111903/files/FNDA2006-058.pdf
17 Y. Y. Pei, Y. B. Zou, Z. Y. Guo, G. Y. Tang, J. G. Xu, J. M. Guo, G. H. Zhang, and L. A. Guo, Nuclear Techniques, **30**: 265 (2007)
18 M. J. Saltmarsh, C. A. Ludemann, C. B. Fulmer, and R. C. Styles, Nucl. Instrum. Methods, **145**: 81 (1977)
19 H. B. Ding, N. Y. Wang, Neutron Source Physics, (Beijing: Science Press, 1984)
20 J. F. Ziegler, M. D. Ziegler, and J. P. Biersack, Nucl. Instrum. Methods Phys. Res. B, **268**: 1818 (2010)
21 D. J. Malbrough, D. K. Brice, D. F. Cowgill, J. A. Borders, L. A. Shope, and J. M. Harris, Nucl. Instrum. Methods Phys. Res. B, **28**: 459 (1987)
22 M. Bader, R. E. Pixley, F. S. Mozer, and W. Whaling, Phy. Rev., **103**: 32 (1956)
23 A. J. Koning, S. Hilaire, and S. Goriely, TALYS-1.8 User Manual, (2015)
24 Y. Iwamoto, Y. Sakamoto, N. Matsuda, Y. Nakane, K. Ochiai, H. Kaneko, K. Niita, T. Shibata, and H. Nakashima, Nucl. Instrum. Methods Phys. Res. A, **598**: 687 (2009)
25 D. Sato, T. Kurosawa, T. Sato, A. Endo, M. Takada, H. Iwase, T. Nakamura, and K. Niita, Nucl. Instrum. Methods Phys. Res. A, **583**: 507 (2007)
26 H. J. Brede, G. Dietze, K. Kudo, U. J. Schrewe, F. Tancu, and C. Wen, Nucl. Instrum. Methods Phys. Res. A, **274**: 332 (1989)